Acta Oceanol. Sin., 2018, Vol. 37, No. 11, P. 19–25
DOI: 10.1007/s13131-018-1293-2
http://www.hyxb.org.cn
E-mail: hyxbe@263.net

Characteristics analysis for cold water patches off the Jiangsu coast in the last 35 a

ZHU Shouxian[1]*, HE Zhanyuan[1], ZHANG Wenjing[2], XIE Shijian[3], XU Yucheng[1]
[1] College of Oceanography, Hohai University, Nanjing 210098, China
[2] College of Meteorology and Oceanography, National University of Defense Technology, Nanjing 211101, China
[3] Zhejiang Surveying of Estuary and Coast, Hangzhou 310008, China

Received 22 November 2017; accepted 28 December 2017

Abstract
The daily and monthly-mean characteristics of cold water patches (CWPs) off the Jiangsu coast in 35 a of 1982–2016 are examined based on advanced very high resolution radiometer (AVHRR) data. Most of the CWPs are found to occur in the warm and hot months (May–September), with some CWPs in the cool and cold months (October–April). The average radius and intensity of the monthly-mean CWPs are about 81 km and 0.6°C, respectively. The average difference in the sea surface temperature (SST) between the centers of the CWPs and the nearshore is about 2.0°C. The correlation analysis between the CWPs, winds and tides indicates that most of the CWPs occurred during the southerly winds, with some CWPs occurring during the northerly winds. The average intensity of the CWPs during spring tides is slightly stronger than that during neap tides in the warm and hot months, and the difference is very small in the cool and cold months.

Key words: Jiangsu coast, cold water patch, characteristic analysis, wind, tide

Citation: Zhu Shouxian, He Zhanyuan, Zhang Wenjing, Xie Shijian, Xu Yucheng. 2018. Characteristics analysis for cold water patches off the Jiangsu coast in the last 35 a. Acta Oceanologica Sinica, 37(11): 19–25, doi: 10.1007/s13131-018-1293-2

1 Introduction

The Jiangsu coast (known as the Subei coast) is the east shore of Jiangsu Province to the southwest of the Yellow Sea and to the north of the Changjiang Estuary. Coastal waters off the Jiangsu coast contain the important fishing ground of Lüsi of China. Previous studies demonstrated that cold water patches (CWPs) occur frequently off the Jiangsu coast, which significantly impact the fisheries (Zhang and Zheng, 1984), the ecological environment (Wei et al., 2011), and concentrations of zooplankton (Liu et al., 2015) and green macroalgae (Li et al., 2015) in the region.

Several studies were made on the characteristics and mechanisms of the CWPs off the Jiangsu coast. Pu (1986) found the occurrence of CWPs from the field observational data collected during the late spring and early summer of 1959 and also from 1975 to 1981. The main physical processes for these CWPs were thought to be the southward migration and climbing up against the slope of deep cold waters from the southwestern part of the Yellow Sea (Pu, 1986). Su and Su (1996) examined the remote sensing data of sea surface temperature (SST) from 1984 to 1987, and concluded that the CWPs were mainly induced by wind-tide mixing and submarine slope. Qi and Su (1998) conducted a numerical simulation of the tide-induced continental front in summer in the Yellow Sea, and found that the mixing by M_2 tidal constituent can lead to the generation of cold waters off the Jiangsu coast. Zou et al. (2001) suggested that the cold waters off the Jiangsu coast in July 1997 and August 1998 were induced by tidal mixing. Lü et al. (2010) used a coupled wave-tide-circulation numerical model to study the summertime circulation in the Yellow Sea. Their model results suggest that tides play three roles in the formation of cold waters off the Jiangsu coast. First, the tide-induced residual current generates barotropic upwelling. Second, the tidal mixing directly reduces the SST. Third, the tidal mixing front induces baroclinic upwelling. Lü et al. (2010) also found that the southerly winds have a less important effect on upwelling than the tidal mixing, and hardly make cold waters without the tidal mixing. The circulation off the Jiangsu coast was traditionally thought to flow southward all the year round (Guan, 1994), but Li (2010) and Yuan et al. (2017) found the northward current using the Lagrangian trajectories of satellite-tracked Argos surface drifters in the summer of 2009 under the forcing of a southerly monsoon, and their numerical experiments with a Princeton ocean model (POM) suggest that the upwelling and cold water off the Jiangsu coast are mainly induced by the southerly wind.

It should be noted that the previous studies focused on the CWPs off the Jiangsu coast in summer and late spring. Examinations of the CWPs in other seasons have not been made. The research on the daily characteristics of the CWPs also remains to be done. The main objectives of this study are to analyze the monthly and daily characteristics of the CWPs in the last 35 a (1982–2016) and to conduct a correlation analysis of the CWPs with winds and tides.

2 CWPs from AVHRR and field observation in July 2016

In this study, we use the daily SST data with a resolution of 0.25°×0.25° from NOAA's AVHRR on polar orbiting satellite to in-

Foundation item: The National Natural Science Foundation of China under contract Nos 41076048, 41376012 and 41206163; the Fundamental Research Funds for the Central Universities under contract No. 2011B05714.
*Corresponding author, E-mail: zhushouxian@vip.sina.com

dicate the characteristics of the CWPs. The observed data from ships and buoys are also syncretized in the AVHRR data. The AVHRR SST data have widely been used in many previous studies (Bao et al., 2002; Lü et al., 2006; Reynolds et al., 2007; Winter and Arkhipkin, 2015; Costoya et al., 2015). The monthly mean SST field from the AVHRR in July 2016 is presented in Fig. 1, which indicates a CWP with a center at about 33.46 °N and 122.42 °E. The SST at the center was 1.2°C lower than that of the outermost enclosed isotherm, and 2.9°C lower than that at the nearshore with the same latitude of the center. The average radius of the outermost enclosed isotherm was about 83.7 km.

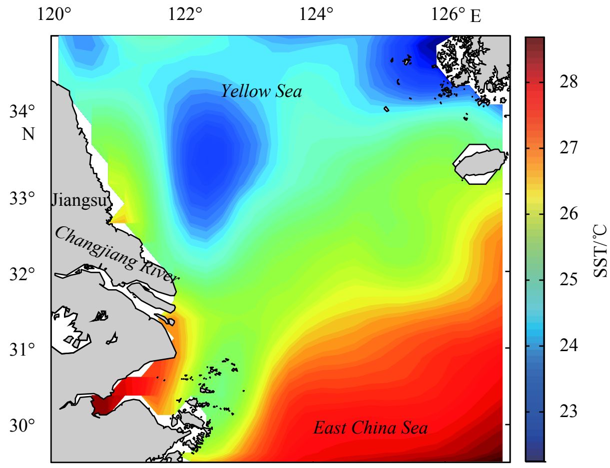

Fig. 1. Monthly mean SST in July 2016 from AVHRR data.

The sea temperature data by a field program in July 2016 are also used in this study to examine the main characteristics of the cold waters, and to demonstrate the ability of the AVHRR data in describing the CWPs. As shown in Fig. 2, the cruise survey along Sections A to C was carried out by a team from Hohai University on 18–21 July, and the survey along Sections D to K by the researchers from East China Normal University on 19–28 July. A conductivity-temperature-depth (CTD) instrument was used in the field program for measuring the vertical profiles of water temperature and salinity. Figure 2a demonstrates that cold waters at a depth of 5 m occur near Sta. A4, which is a location similar to that of the CWP depicted in Fig. 1. As shown in Figs 2b–f, the main axis of cold waters tilted to the east at deeper depths, with their centers at 10 m near Sta. A4, at 15 m near Sta. A5, and at 25 m near Sta. A6. Figure 2 also indicates that Section A crosses approximately the cold waters. The vertical distribution of the water temperature along Section A is presented in Fig. 3. Along this section, waters were well mixed with nearly uniform temperature in the vertical to the west of Sta. A3. There was a cold water tongue reaching the surface near Sta. A4, which was from the eastern deep waters. It is demonstrated again that the cold waters are accompanied by upwelling from the Yellow Sea as reported in previous studies (Lü et al., 2010; Li, 2010; Yuan et al., 2017). The waters to the east of Sta. A5 had a three-layer structure of the upper mixed layer, thermocline, and lower mixing layer. The thicknesses of the upper mixed and thermocline layers were both nearly 10 m.

3 Characteristic analysis of monthly mean CWPs by AVHRR data in the last 35 a

The ranges and centers of the CWPs can not easily be determined if there are no closed isotherms. In this study, we focus mainly on the CWP which has a SST difference of 0.2°C (or greater than that value) between its center and the outermost enclosed isotherm. Furthermore, the positions of the cold centers are restricted to the domain of 32°–34°N, 121°–124°E. Four parameters are used to describe the characteristics of each CWP: its center position, radius, intensity, and the SST difference between the cold center and nearshore at the same latitude (SSTD-CN). The radius of the CWP is defined as the mean radius of the outermost enclosed isotherm, and the intensity of the CWP is defined as the SST difference between the center and outermost enclosed isotherm.

Table 1 lists 146 CWPs determined from the monthly mean SSTs in the 35 a period of 1982–2016. The total number of the CWPs in each year varies, with a maximum of seven in 2003 and a minimum of three in 10 different years. The centers of the CWPs are marked in Fig. 4, with water depths represented by the color image. The centers of most CWPs were located to the east of 122°E, where the terrain is a shelf slope with water depths of 20–40 m. By comparison, the centers of two CWPs were in the shore shoal, where the water depth is less than 20 m. One of the CWPs was detected in January 2003 and the other in December 2003. Figure 5a shows the distribution of CWP radii. The CWP radii were 32–168 km with an average value of about 81 km. Nearly 80% of CWPs had radii of 32–109 km. The distribution of the CWP intensity is shown in Fig. 5b. The values of the CWP intensity varied in the range 0.2–1.5°C with an average of 0.6°C. The SSTD-CNs (Fig. 5c) were 0.2–4.2°C with an average of 2.0°C, and about 89% of them were in the range 0.6–3.0°C. The CWP in June 1988 had the largest radius of 168 km, with an intensity of 1.2°C and an SSTD-CN of 2.2°C. The CWP in this month was in the shape of an ellipse extending from southeast to northwest, and nearly covered the entire Jiangsu coast (Fig. 6).

The statistics for the seasonal variation of the monthly mean CWPs from 1982 to 2016 are given in Table 2. In the cold months (December–February) of winter, there were only two CWPs, while in the cool months (including March, April, October and November), there were 16 CWPs. Twenty eight CWPs occurred in the warm months (May and September) of late spring and early autumn. There were 100 CWPs in the hot months (June to August) of all 35 a, and no CWPs were detected in only five of these months. In general, the CWPs in the warm and hot months had stronger intensities, larger radii and SSTD-CNs than those in the cold and cool months.

4 Characteristic analysis of daily CWPs by AVHRR data from 2001 to 2010

The AVHRR data in the 10 a period of 2001–2010 were used to analyze the characteristics of daily CWPs. The seasonal variations in the total number of days, average intensity, and maximum intensity of daily CWPs are given in Fig. 7. The total number of daily CWPs was 1 369, which was about 38% of the total days in this 10 a period. The CWPs occurred in about 12% of the days of cold months, 21% of the days of cool months, and 66% of the days of warm and hot months. By comparison, the CWPs occurred in 82% of the summer days. Of the 12 months, the daily CWPs in July had the largest number of 273, the strongest average intensity of 1.0°C and maximum intensity of 2.4°C.

As shown in Table 1, the least monthly mean CWPs were detected in 2001 and the most in 2003. The distributions of daily CWPs in 2001 and 2003 are plotted in Fig. 8. The monthly mean CWPs only occurred in May, June, and July 2001, while the numbers of daily CWPs were 3, 0, 2, 3, 21, 21, 31, 28, 11, 2, 0 and 0 from January to December, respectively, and the longest duration of

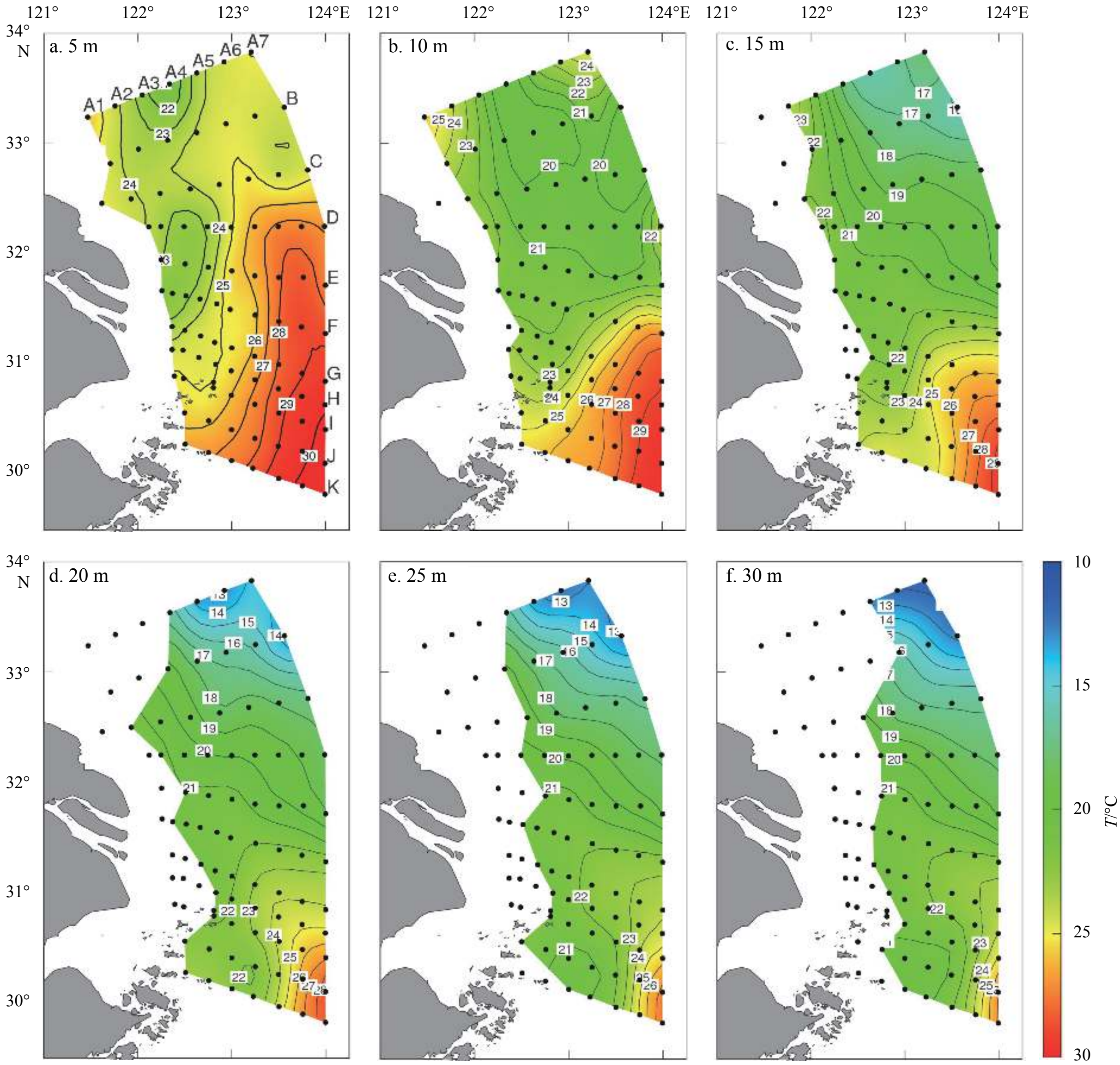

Fig. 2. Water temperatures at different depths constructed from *in situ* observations in July 2016.

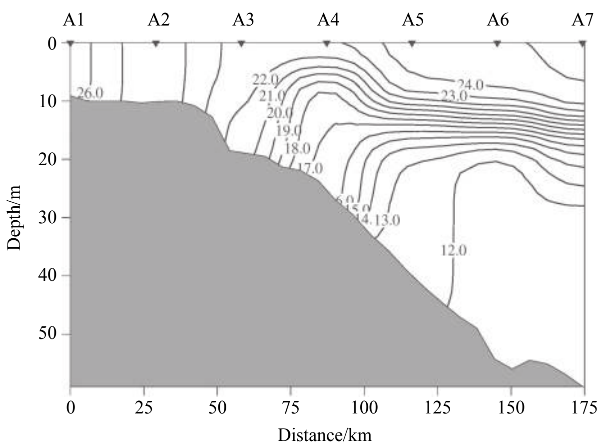

Fig. 3. Vertical distribution of water temperature (°C) along Section A in July 2016.

the CWP was 51, from June 27 to August 16. The monthly mean CWPs were found in January, April, May, June, July, August and December 2003; the total numbers of daily CWPs were 23, 6, 11, 22, 21, 30, 29, 29, 0, 5, 12 and 30 from January to December 2003, respectively; and the longest duration of the CWP was 56 days, from May 29 to July 22. Figure 8 also indicates that the generations and extinctions of daily CWPs were quick. Some daily CWPs may generate and become strong in 1 day and some strong CWPs may die out in 1 day. There were quite a number of daily CWPs in some months of 2001 and 2003, but their centers and shapes were so different that they were smoothed out in the monthly mean fields, leading to no monthly mean CWPs. For example, there were 28 daily CWPs in August 2001 with an average intensity of 0.9°C, but their centers occurred in different places (Fig. 9), so there were only cold waters in the monthly mean SST (Fig. 10) that did not meet the standard of a CWP in the domain of 32°–34°N and 121°–124°E.

5 Correlations between CWPs, wind forcing and tides

The wind forcing and tides were thought to have important effects on the CWPs (Pu, 1986; Su and Su, 1996; Qi and Su, 1998; Zou et al., 2001; Lü et al., 2010; Li, 2010; Yuan et al., 2017). In this study, we analyzed the correlations of the CWPs, wind forcing

Table 1. CWPs determined from monthly mean SSTs of AVRHH data from 1982 to 2016

Year	Months when CWP existed	Year	Months when CWP existed	Year	Months when CWP existed	Year	Months when CWP existed
1982	6, 7, 9	1991	5, 6, 7, 8, 9	2000	3, 6, 8	2009	4, 6, 7, 8, 9
1983	6, 7, 8, 10	1992	6, 7, 8	2001	5, 6, 7	2010	3, 6, 7, 8
1984	5, 6, 7, 8, 10	1993	6, 7, 8, 9, 10	2002	6, 7, 8	2011	5, 6, 7, 8
1985	4, 5, 6, 7, 8	1994	4, 6, 7, 8, 9	2003	1, 4, 5, 6, 7, 8, 12	2012	4, 6, 7, 8
1986	5, 6, 7, 8	1995	5, 6, 7, 8	2004	4, 6, 7, 9	2013	6, 7, 8, 9
1987	6, 7, 8, 9	1996	5, 6, 7, 8, 9	2005	6, 7, 8	2014	5, 6, 7, 8, 9
1988	4, 6, 7, 8, 9	1997	6, 7, 8	2006	6, 7, 8, 9, 10	2015	5, 6, 7, 8
1989	4, 5, 6, 7, 8	1998	6, 7, 8, 9	2007	6, 7, 8	2016	4, 6, 7, 8
1990	7, 8, 9	1999	4, 5, 6, 7, 8, 9	2008	6, 7, 8		

Note: The numbers of 1–12 represent January to December respectively.

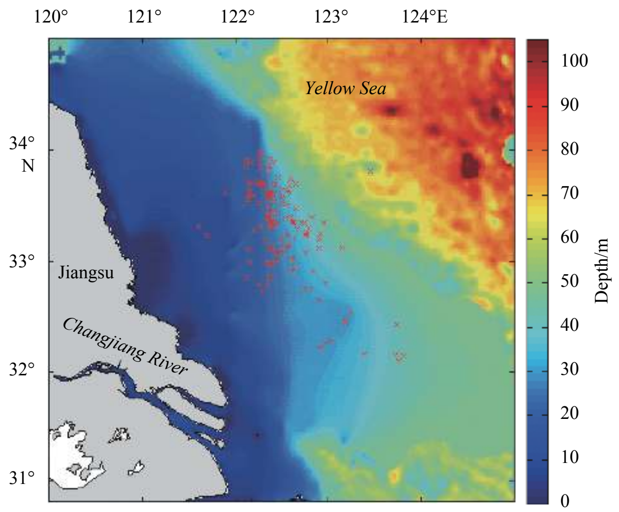

Fig. 4. Centers of monthly mean CWPs from 1982 to 2016 (the red asterisks represent the positions of centers).

and tides in the last 35 a. The wind data were from the European Centre for Medium-range Weather Forecasts (ECMWF), which were at height of 10 m on the sea surface with a spatial resolution of 0.25°×0.25° and a time resolution of 6 h. The wind data were spatially averaged in the domain of 32°–34°N and 121°–124°E. The tide data were from the ocean tide model of DTU10 developed by the Technical University of Denmark (Cheng and Andersen, 2011).

The time-averaged winds in all days from 1982 to 2016 are presented in Fig. 11a, together with the time-averaged wind only when monthly mean CWPs existed (Fig. 11b). Since no monthly mean CWPs occurred in February and November (Table 2), the time-averaged winds in these two months are not shown in Fig. 11b.

An examination of Fig. 11a and Table 2 indicates that the southerly components of the time-averaged winds increase from January to July, and the total number, average intensity, average radius, and average SSTD-CN of the monthly mean CWPs, in general, also increase. In January, March, September, October and December, however, the time-averaged winds when monthly mean CWPs existed were northerly (Fig. 11b). From May to August, although the time-averaged winds when the monthly mean CWPs existed were southerly, they did not have obviously stronger southerly constituents than those in all days.

The quick generations and extinctions of the daily CWPs (Fig. 8) indicate that the daily winds may have more direct correlations with the daily CWPs. Table 3 gives the time-averaged winds in the all days and those when the daily CWPs existed from 2001 to 2010. In the all months (January–December), the time-averaged wind in the all days was northerly, while the time-averaged wind when the daily CWPs existed was southeasterly. There were daily CWPs in most days of summer, but there were no daily CWPs in most days of winter, it is necessary to make further comparisons between the daily winds and CWPs in different months. In the warm and hot months (May–September), the southerly constituent of the time-averaged wind when the daily CWPs existed was 150% of that in the all days. Of the 1003 daily CWPs in the warm and hot months, 525 daily CWPs corresponded to v (the longitudinal component of wind) beyond its average value of 1.2 m/s, and they had an average intensity of 0.9°C. The other 478 daily CWPs had an average intensity of 0.6°C. It seems that larger amount and stronger intensity of the daily CWPs corresponded to stronger southerly constituent of wind. The time-averaged wind when the daily CWPs existed had the northerly constituent of –1.3 m/s in the cool months (March, April, October and November), and the northerly constituent of –3.6 m/s in the cold months (December–February).

As shown in Fig. 4, most CWPs had the centers around 33.5°N

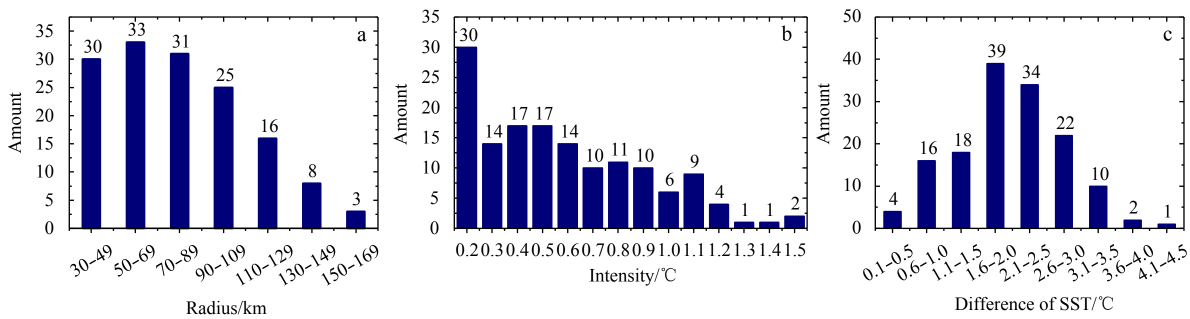

Fig. 5. Characteristics of monthly mean CWPs from 1982 to 2016 in terms of the radius (a), intensity (b) and SSTD-CN (c).

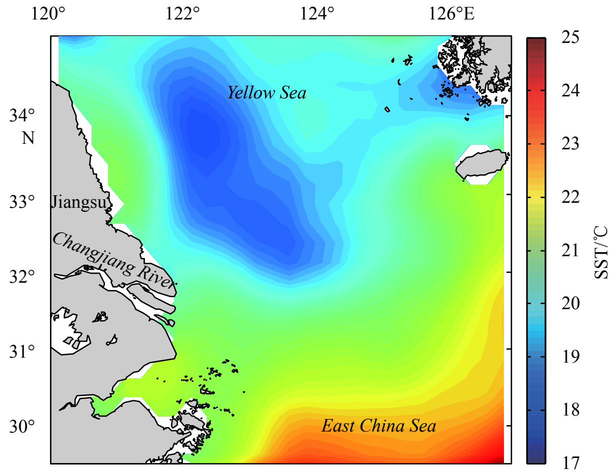

Fig. 6. Monthly mean CWP calculated from AVRHH data in June 1988.

Table 2. Seasonal variations of monthly mean CWPs from 1982 to 2016

Month	Amount of CWPs	Average intensity/°C	Average radius/km	Average SSTD-CN/°C
Jan.	1	0.5	58	0.8
Feb.	0	–	–	–
Mar.	2	0.2	37	0.2
Apr.	10	0.3	54	1.2
May	13	0.4	58	2.1
Jun.	34	0.6	74	2.1
Jul.	34	0.8	97	2.5
Aug.	32	0.7	95	2.3
Sep.	15	0.4	74	1.5
Oct.	4	0.2	50	0.7
Nov.	0	–	–	–
Dec.	1	0.6	62	0.8

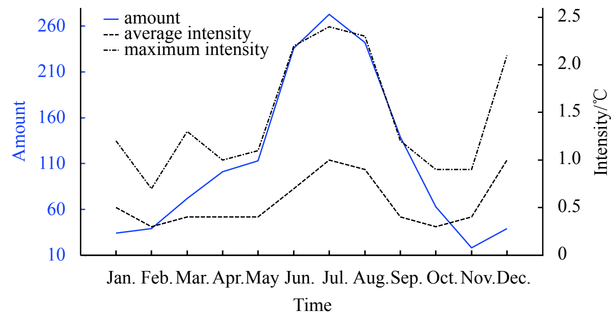

Fig. 7. Seasonal variations of daily CWPs in the 10 a period of 2001–2010.

and 122.5°E, The tide level at this station was selected to represent the tidal variation off the Jiangsu coast. The average value of tidal range was 257 cm during spring tides and 113 cm during neap tides from 2001 to 2010. The tidal ranges at this location varied significantly from the neap tide to spring tide. There were 243 spring tides from 2001 to 2010, and 3 d of every spring tide were picked out to constitute the spring tide period. The neap tide period was constituted by the similar way. The statistics of daily CWPs during the spring and neap tide periods are given in

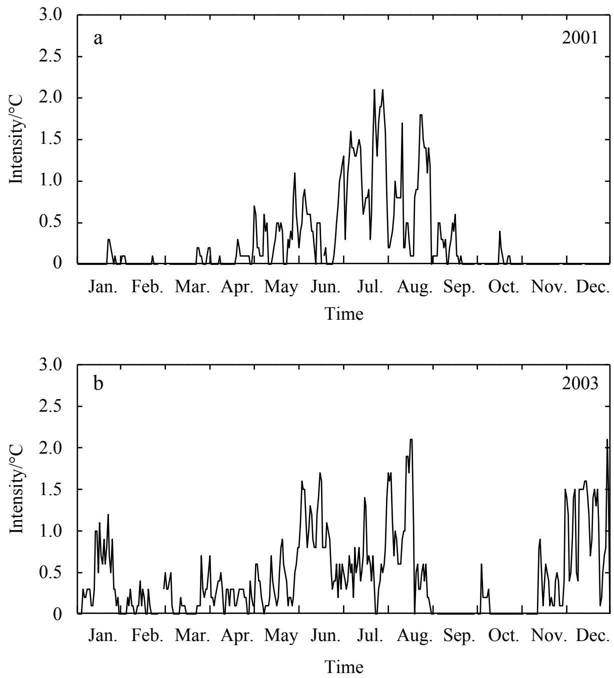

Fig. 8. Intensity of daily CWPs in 2001 (a) and 2003 (b).

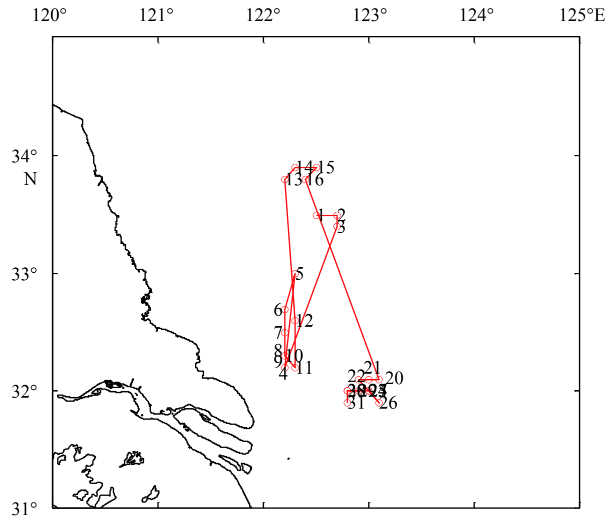

Fig. 9. Centers of daily CWPs in August 2001 (the numbers represent dates of the month).

Table 4. In the all months (January–December), the daily CWPs during the spring tide period were 107% of those during the neap tide period. And the average intensity of daily CWPs during the spring tide period was 0.1°C stronger than that during the neap tide period. In the warm and hot months (May–September), the daily CWPs during the spring tide period were 112% of those during the neap tide period. In the cold and cool months (October–April), the total number of the daily CWPs during the spring tide period was 7 less than that during the neap tide period, the averaged intensity of daily CWPs during the spring tide period was nearly same as that during the neap tide period.

6 Discussion and conclusions

Both the AVHRR SST data and the *in situ* oceanographic ob-

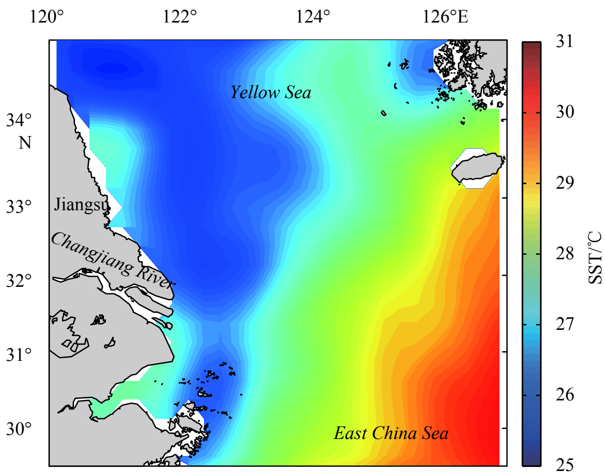

Fig. 10. Monthly mean SST in August 2001.

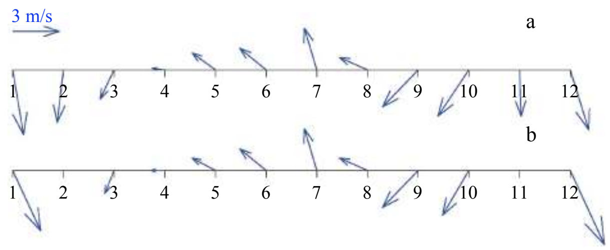

Fig. 11. The time-averaged wind velocities in all days (a) and when monthly mean CWPs appeared (b). The numbers of 1 to 12 represent January to December, respectively.

servations in July 2016 were found to support the existence of CWPs off the Jiangsu coast. This indicates that the AVHRR SST data can perform reasonably well in describing the CWPs. In the last 35 a (1982–2016), there have been 146 monthly mean CWPs in the AVHRR SST data, 128 of them existed in the warm and hot months (May–September). The daily CWPs occurred in 66% of the days of warm and hot months. Therefore, the CWPs are the common hydrographic phenomena in the warm and hot months in the past 35 a. However, some CWPs were also found during the cool and cold months (October–April), which were not presented previously.

The effects of southerly winds and tides on the CWPs were studied previously. The Jiangsu coast lies east of the continent of Asia in the Northern Hemisphere, and is roughly in the north-south direction. The ocean currents in the upper waters off the Jiangsu coast induced by the southerly winds turn offshore (eastward) due to the impact of the Coriolis force. Compensation currents in the lower waters flow shoreward (westward), and are raised by the shelf slope to form the coastal upwelling. Several previous studies (Li, 2010; Yuan et al., 2017) suggested that the cold waters off the Jiangsu coast in summer are mainly induced by southerly winds. The tides in the region can mix the waters vertically. The waters over the shore shoal and shelf slope were found to be well mixed, while waters over the deep offshore were partially mixed, thus the water temperature over the shelf slope should be lower than those over the shore shoal and deep offshore. The tidal mixing was thought to be the main dynamic of cold water off the Jiangsu coast in other studies (Qi and Su, 1998; Zou et al., 2001). It was further found that the tidal mixing front can induce baroclinic upwelling to form cold water (Lü et al., 2010). In the studies of low salinity water lens in the Changjiang River diluted water expansion, the tidal mixing and its increase from the neap tide to spring tide were also found to have significant effect on the hydrodynamics off the Jiangsu coast (Zhang et al., 2014; Peng et al., 2014). In this study, the correlation analysis indicates that the larger amount and stronger intensity of the daily CWPs generally corresponded to stronger southerly constituent of wind, and the daily CWPs during the spring tide period have slightly larger amount and stronger average intensity than those during the neap tide period in the warm and hot months (May–September).

The correlation characteristics of CWPs, winds and tides also indicate that some CWPs need further studies. First, although most CWPs correspond to southerly winds from May to August, the southerly components of time-averaged winds when the monthly mean CWPs exist are not stronger than those without monthly mean CWPs (Fig. 11). While in Table 3, the larger amount and stronger intensity of the daily CWPs correspond to stronger southerly constituent of wind in warm and hot months. Therefore, the monthly mean wind may not be a good indicator as the daily wind in illustrating the effects of winds on the CWPs. More studies are still needed to determine any additional explanations for the effects of southerly winds. Second, there are also some daily and monthly mean CWPs corresponding to northerly winds. One of important issues to be addressed is the effect of

Table 3. Correlation between wind and daily CWPs from 2001 to 2010

Month	Amount of all days	Time-averaged wind of u, v in all days	Days when CWPs existed	Time-averaged wind of u, v when CWPs existed
Jan. – Dec.	3 652	−0.8, −1.1	1 369	−1.4, 0.4
May – Sep.	1 530	−1.7, 0.8	1 003	−1.6, 1.2
Mar., Apr., Oct., Nov.	1 220	−0.6, −1.7	254	−1.0, −1.3
Jan., Feb., Dec.	902	0.3, −3.7	112	0.1, −3.6

Note: u and v represent the latitudinal and longitudinal components of wind velocities (m/s), respectively.

Table 4. Statistics of CWPs during spring and neap tides from 2001 to 2010

Month	During spring tide period		During neap tide period	
	Days when CWPs existed	Average intensity of CWPs/°C	Days when CWPs existed	Average intensity of CWPs/°C
Jan. – Dec.	281	0.7	266	0.6
May – Sep.	208	0.8	186	0.7
Jan., Feb., Dec.	18	0.5	20	0.5
Mar., Apr., Oct., Nov.	55	0.4	60	0.4

northerly wind on the CWPs in the study region. Third, although the average tidal range during spring tides is nearly twice of that during neap tides, but the averaged intensity of the daily CWPs during spring tides is only slightly stronger than that during neap tides in the warm and hot months (May–September), and they nearly have no difference in the cool and cold months (October–April). The tidal range during neap tide may be strong enough to well mix up the water columns and produce the CWP. Are there any other explanations for the effects of tide? Finally, in the dynamical explanations of the CWP using the upwelling and mixing, the vertical temperature stratification is a precondition. The stratification over the Yellow Sea and Jiangsu coast generally increase from winter to summer (Diao, 2015), which agree with most CWPs appearing in the warm and hot months. While there are also considerable amount of monthly mean and daily CWPs exist in the cool and cold months. Was the stratification considerable strong when the CWPs occurred in the cool and cold months? Or can the CWPs be explained by any dynamics different from upwelling and mixing? But the data analysis in this study is difficult to answer these questions. We want to make further dynamical analysis on these CWPs using numerical simulations in the future.

References

Bao Xianwen, Wan Xiuquan, Gao Guoping, et al. 2002. The characteristics of the seasonal variability of the sea surface temperature field in the Bohai Sea, the Yellow Sea and the East China Sea from AVHRR data. Haiyang Xuebao (in Chinese), 24(5): 125–133

Cheng Y, Andersen O B. 2011. Multimission empirical ocean tide modeling for shallow waters and polar seas. Journal of Geophysical Research: Oceans, 116(C11): C11001

Costoya X, deCastro M, Gómez-Gesteira M, et al. 2015. Changes in sea surface temperature seasonality in the Bay of Biscay over the last decades (1982–2014). Journal of Marine Systems, 150: 91–101

Diao Xinyuan. 2015. The study of Yellow Sea Warm Current, Yellow Sea cold water mass and their evolution process in spring (in Chinese)[dissertation]. Guangzhou: Institute of Oceanology, Chinese Academy of Science

Guan Bingxian. 1994. Patterns and structures of the currents in Bohai, Huanghai and East China Seas. In: Zhou Di, Liang Yuanbo, Zeng Chengkui, eds. Oceanology of China Seas. Dordrecht: Springer

Li Yao. 2010. Structure and dynamics of ocean circulation off the East Coast of China (in Chinese) [dissertation]. Guangzhou: Institute of Oceanology, Chinese Academy of Sciences

Li Yuesong, Xiao Wenjun, Yang Hong, et al. 2015. Dynamic analyses of early development and gather of green macroalgae in 2012. Marine Environmental Science (in Chinese), 34(2): 268–273

Liu Guangxin, Kong Wei, Yang Guipeng. 2015. Influence of tidal front on distribution of paracalanus parvus and chlorophyll a in summer over South Yellow Sea. Oceanologia et Limnologia Sinica (in Chinese), 46(1): 58–64

Lü Xingang, Qiao Fangli, Xia Changshui, et al. 2006. Upwelling off Yangtze River estuary in summer. Journal of Geophysical Research: Oceans, 111(11): C11S08

Lü Xingang, Qiao Fangli, Xia Changshui, et al. 2010. Upwelling and surface cold patches in the Yellow Sea in summer: effects of tidal mixing on the vertical circulation. Continental Shelf Research, 30(6): 620–632

Peng Jian, Zhu Shouxian, Li Xunqiang, et al. 2014. Impact of wind on the low-salinity water lens in the northeast out of the Changjiang estuary in summer. Journal of East China Normal University (in Chinese), (3): 105–116

Pu Yongxiu. 1986. Cold water areas on the sea surface off Subei in late spring and summer. Oceanologia et Limnologia Sinica (in Chinese), 17(5): 453–457

Qi Jianhua, Su Yusong. 1998. Numerical simulation of the tide-induced continental front in the Yellow Sea. Oceanologia et Limnologia Sinica (in Chinese), 29(3): 247–254

Reynolds R W, Smith T M, Liu Chunying, et al. 2007. Daily high-resolution-blended analyses for sea surface temperature. Journal of Climate, 20(22): 5473–5496

Su Yusong, Su Jie. 1996. The preliminary analysis of the cold water zones and their mechanisms during summer in the Bohai Sea and Yellow Sea. Acta Oceanologica Sinica (in Chinese), 18(1): 13–20

Wei Qinsheng, Zang Jiaye, Zhan Run, et al. 2011. Characteristics of the ecological environment in the upwelling area northeast of the Changjiang River Estuary. Oceanologia et Limnologia Sinica (in Chinese), 42(6): 899–905

Winter A, Arkhipkin A. 2015. Environmental impacts on recruitment migrations of Patagonian longfin squid (Doryteuthis gahi) in the Falkland Islands with reference to stock assessment. Fisheries Research, 172: 85–95

Yuan Dongliang, Li Yao, Wang Bin, et al. 2017. Coastal circulation in the southwestern Yellow Sea in the summers of 2008 and 2009. Continental Shelf Research, 143: 101–117

Zhang Rui'an, Zheng Dong. 1984. The spring Yellow Sea oceanic fronts and their relations to fisheries. Marine Science (in Chinese), 8(1): 5–8

Zhang Wenjing, Zhu Shouxian, Li Xunqiang, et al. 2014. Numerical simulation and dynamical analysis for low salinity water lens in the expansion area of the Changjiang diluted water. China Ocean Engineering, 28(6): 777–790

Zou Emei, Guo Binghuo, Tang Yuxiang, et al. 2001. An analysis of summer hydrographic features and circulation in the southern Yellow Sea and the northern East China Sea. Oceanologia et Limnologia Sinica (in Chinese), 32(3): 340–348